Proceedings of the 21st International Conference on Global Research and Education (Inter-Academia 2024)

Parameter Evaluation of Three-Point Step Control System

J. Możaryn* and P. Rył

Faculty of Mechatronics, Institute of Automatic Control and Robotics, Warsaw University of Technology, św. A. Boboli 8, 02-525 Warsaw, Poland

Doi: 10.12693/APhysPolA.146.399 *e-mail: jakub.mozaryn@pw.edu.pl

The three-point controller is one of the simplest controllers used in industry. Most environments with programmable logic controllers and distributed control systems allow such blocks in their design. The three-point controller consists of three switching states, i.e., one input and two outputs, depending on the input signal's positive or negative deviation from the desired value. It allows for an upper and lower limit of deviation where no switching takes place. The three-point step control system extends the step controller with a corrective feedback loop. This paper presents the implementation and parameter evaluation of the three-point step control system. Based on theoretical analysis and simulations, general comments are made on the impact of the controller parameters on the control system's performance. Finally, recommendations for tuning the three-point step controller are formulated.

topics: three-point (3P) step control, controller tuning, controller design

1. Introduction

The three-point (3P) controller is one of the simplest controllers used in industry. Most environments with *programmable logic controllers* (PLC) and *distributed control systems* (DCS) allow such blocks in their design [1]. The 3P controller consists of three switching states, i.e., one input and two outputs, depending on a certain positive or negative deviation of the input signal from the desired value. It allows the switching of two different types of energy and usually includes a gain parameter with upper and lower limits of deviation at which no switching takes place.

The three-point step (3P-S) controller is an extension of the 3P controller with a corrective feedback loop. Technical solutions using the 3P-S controller include automatic pressure control systems [2], refrigerant flow control systems in scroll compressors [3], automatic temperature control systems [4], and *pulse-width modulation* (PWM) rectifiers [5]. The 3P-S control algorithm is particularly useful for controlling drive systems where rotational or linear motion in both directions is required [6, 7]. The main advantage of the 3P-S control system is that the controller outputs are digital, which reduces the cost due to the absence of elements controlled by an analogue signal. However, the obvious disadvantage of such implementations is higher power consumption compared to *proportional–integral–derivative* (PID) controllers [8].

2. The 3P-S controller

The 3P controller has three states, depending on the size of the control deviation, e. It is described by the following equation [9]

$$x = f\left(e\right) = \begin{cases} -B & \text{for } e < a, \\ 0 & \text{for } |e| \le a, \\ +B & \text{for } e > a, \end{cases} \tag{1}$$

where: x — control variable, B — power factor, a — deadband.

Usually, an additional hysteresis band h is introduced into the system, defined as the difference between the value of control deviation for which the state of the output from the controller changes depending on the previous state [10] (see Fig. 1). In

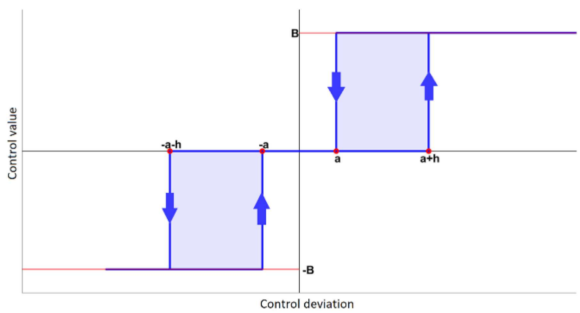

Fig. 1. The 3P controller characteristics.

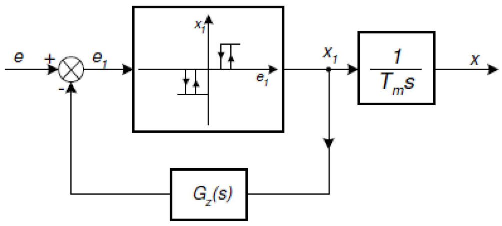

Fig. 2. The block diagram of the 3P-S controller [9].

such a case, the transition from the state '0' to the states '$\pm B$' takes place for the control deviation value equal to $|a+h|$, and the return from the states '$\pm B$' to the state '0' takes place for the control deviation value equal to $|a|$. This can be written as

- for $\mathrm{sign}(\frac{\mathrm{d}}{\mathrm{d}t} e(t)) > 0$

$$x = f(e) = \begin{cases} -B & \text{for } e \le -a, \\ 0 & \text{for } -a < e \le a+h, \\ +B & \text{for } e \ge a+h, \end{cases} \tag{2}$$

- for $\mathrm{sign}(\frac{\mathrm{d}}{\mathrm{d}t} e(t)) < 0$

$$x = f(e) = \begin{cases} -B & \text{for } e \le -a-h, \\ 0 & \text{for } -a-h < e \le a, \\ +B & \text{for } e \ge a. \end{cases} \tag{3}$$

However, the 3P controller with hysteresis does not achieve satisfactory control results for higher-order processes with delays. For such systems, eliminating oscillations requires a significant extension of the deadband, which increases the potential range of steady-state error. To successfully utilize the 3P control algorithm, the controller structure should be modified by incorporating a corrective feedback loop with the transfer function $G_z(s)$. The modified deviation value e_1, which is fed into the controller, enables the process to be influenced by a continuous controller with a structure similar to that of a proportional–integral (PI) controller (see Fig. 2). Additionally, in the implementation of the 3P-S controller, the controller's structure should incorporate an object transfer function in the form of an integrator [9] as

$$\frac{x(s)}{e(s)} = \frac{1}{G_z(s)} \frac{1}{T_m s}, \tag{4}$$

where: $G_z(s)$ — corrective feedback transfer function, T_m — time constant of the plant.

3. Corrective feedback

The corrective feedback transfer function $G_z(s)$ allows the signals from the controller to be alternately positive and negative. In this way, the output signal from the controller will resemble a sawtooth signal, with the average value depending on the value of the control deviation [8]. For the step controller to have properties similar to the PI algorithm, the corrective transfer function must be in the form

$$G_z(s) = \frac{T_i}{k_p T_m (T_i s + 1)} = \frac{k}{T_i s + 1}, \tag{5}$$

where: T_i — time constant of the corrective feedback, k — proportional gain of the corrective feedback.

When selecting the corrective transfer function parameters, it is essential to determine the parameters k and T_i using methods similar to those used for a PI controller, but without actuator dynamics. In addition, understanding the actuator dynamics is necessary to determine the value of T_m. However, the challenge of selecting the parameters for the 3P block (see Fig. 2) remains.

4. Theoretical analysis of the 3P-S controller performance

The boundary value of the steady-state error for the 3P-S controller is expressed as the inequality [11]

$$e_{st} \le 2a, \tag{6}$$

where e_{st} is the steady-state error.

By adjusting the a coefficient, it is possible to limit the magnitude of e_{st}, which almost always occurs in 3P control systems where the response differs from steady oscillations. However, the value of e_{st} within the limit defined by (6) depends on a larger number of parameters.

Another performance index considered is the period of oscillation, T_{osc}. The rise time, t_w, of the output signal from feedback e_1 (see Fig. 2) and the fall time, t_m, of e_1 can be determined separately [11]. It is due to the time the error oscillates in the range from $|a|$ to $|a+h|$.

The sum of the rise and fall times is the oscillation period. The rise time of $e_1(t)$ depends not only on the parameters of the inertial element included in the feedback loop but also on the parameters of the 3P-S controller, and it can be expressed as

$$t_w = \frac{h}{[k e_1'(t)]_w - e(t)} \approx \frac{h T_i}{k B - e(t) - T_i e'(t)}, \tag{7}$$

where $e_1'(t) = \frac{\mathrm{d}}{\mathrm{d}t} e_1(t)$, $e'(t) = \frac{\mathrm{d}}{\mathrm{d}t} e(t)$.

Similarly, the fall time of $e_1(t)$ can be described as

$$t_m = \frac{h}{[k e_1'(t)]_m + e(t)} \approx \frac{h T_i}{e(t) + T_i e(t)}. \tag{8}$$

Therefore, the oscillation period can be expressed by the following equation [11]

$$t_w + t_m = \frac{A h T_i}{\frac{A}{T_1} e - \frac{1}{T_1^2} e^2 + (A T_1 - 2e) e' - T_i^2 (e')^2}, \tag{9}$$

where $A = kB$.

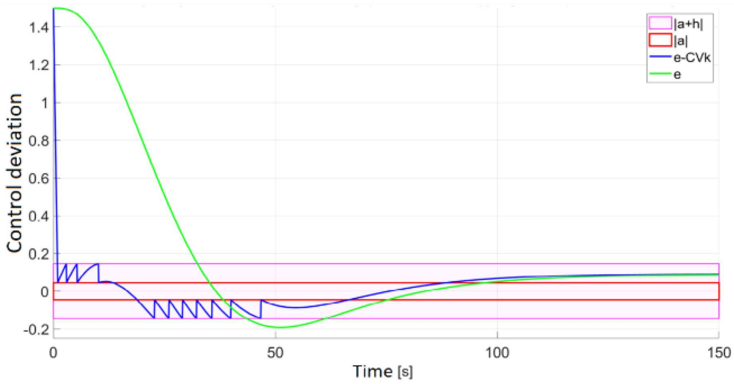

Fig. 3. Characteristic of system deviation e and corrected control deviation.

Using the condition

$$\frac{\partial}{\partial e}(t_w + t_m) = \frac{\partial}{\partial e'}(t_w + t_m) = 0, \tag{10}$$

the following relationship is obtained

$$e = 0.5AT_1 - T_1^2 e'. \tag{11}$$

After substituting (10) in (11), the following relationship can be obtained

$$(t_w + t_m)_{\min} = \frac{4T_1\,h}{k\,B}. \tag{12}$$

By combining (12) and (6), the following parameter can be calculated as

$$k_j = \frac{(t_w + t_m)_{\min}}{e_{st}} \geq \left(\frac{2}{B}\right)\left(\frac{T_i}{k}\right)\left(\frac{h}{a}\right). \tag{13}$$

The parameter k_j helps determine both the adequacy and effectiveness of the controller tuning. A higher value of k_j indicates better controller performance. Reducing the power factor B consistently reduces the overshoot. The corrective feedback ratio ($\frac{T_i}{k}$) depends primarily on the dynamic characteristics of the plant and is determined during tuning. The step ratio ($\frac{h}{a}$) should be maximized because hysteresis affects the stability of the control system. Reducing the width of the deadband a limits the range of possible steady-state error values (6).

Another important metric for evaluating the selected control parameters is the duration of the shortest control pulse. This parameter is crucial when selecting a plant with a correspondingly high cutoff frequency. It can be calculated as follows

$$(t_w)_{\min} = \frac{h\,T_1}{k\,B}. \tag{14}$$

5. Impact of the 3P-S parameters on the control system performance

5.1. Plant

Let us consider an example where the plant is described as a third-order inertial object with an integrator

$$G_{ab}(s) = \frac{1}{2s}\,\frac{8}{18s+1}\,\frac{1}{9s+1}\,\frac{1}{4.5s+1}. \tag{15}$$

Such systems are often encountered in control applications involving mechanical, thermal, or electrical processes where inertia and damping effects are significant [12].

5.2. Principle of operation of the 3P-S controller

In the scenario considered, the system's step response was analysed for a setpoint change with an amplitude of 1.5 (see Fig. 3). The influence of the corrective feedback on the resulting deviation was studied. The corrected deviation value stabilises much faster within the range $a < e < a + h$, effectively limiting the system response's overshoot. The first control pulse occurs when the process variable is less than [8]

$$y = w + a - B\,\frac{T_i}{k_p T_m}, \tag{16}$$

where w is the excitation value.

Thus, both the corrective transfer function parameters (5) and the parameters of the 3P-S controller influence the behaviour of e_1. For the examined plant (15), the parameters of the corrective transfer function (5) were set to $k = 78.37$ and $T_i = 25.66$ s.

Due to the first-order nature of the coupling, the rate of change of the correction signal is influenced by the feedback time constant. A decrease in the correction signal causes an increase in the error e_1 at the controller input, which causes the controller to reset to the ($+B$) state. After correction, the error value oscillates several times between a and $a + h$, generating short pulses in the controlled variable even before the first actual error switching limit is reached [8].

As the controller operates, the corrected deviation error decreases until it finally falls within the deadband of the controller $|a|$; at this point, the controller output switches to the '0' state.

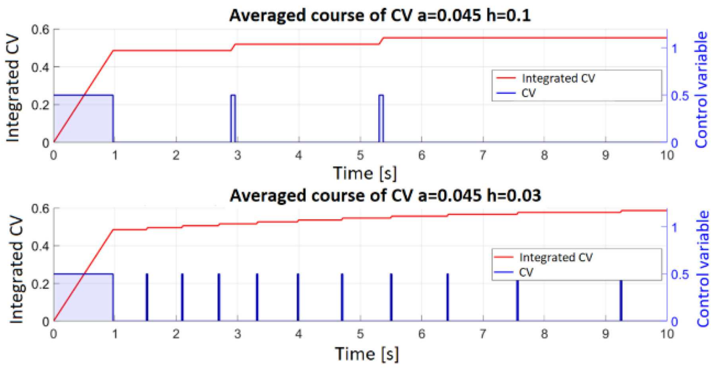

Fig. 4. Comparison of the integrated value of the control variable (CV) for the two values of the hysteresis band.

TABLE I

Performance parameters for a 3P step controller for different settings of deadband and hysteresis.

Power coefficient $B = 005$				
3P-S	$a = 0.105$ $h = 0.05$	$a = 0.15$ $h = 0.05$	$a = 0.105$ $h = 0.1$	$a = 0.15$ $h = 0.1$
$(\frac{h}{a})$	0.48	0.33	0.95	0.67
k_j	6.24	4.37	12.47	8.73
$(t_w)_{\min}$	0.32 s	0.32 s	0.64 s	0.64 s
I_{ISE}	47.46	48.54	48.09	51.58
κ	13.2%	14.59%	13.8%	15.33%
e_{st}	0.003	−0.03	−0.02	−0.11
T_{set}	88.3 s	100.7 s	95.2 s	–*
n_{imp}	11	10	5	4
k_w	4.80%	4.50%	4.50%	4.15%

*Steady-state error was greater than 5% of SP

The correction signal e_1 decreases faster than the actual error e, resulting in a change in the sign of the corrected error. Once the value exceeds $-a$, the controller generates pulses of the opposite sign, which helps limit the overshoot if the control signal remains positive throughout and reduces the likelihood of oscillations in the system response.

By correcting the signal reaching the input of the 3P-S controller, the controller can anticipate further changes in the error. To illustrate the similarities between the step controller and the PI controller, the averaged trajectory of the integrated output is shown in Fig. 4. From this comparison, it can be seen that there is a direct relationship between the hysteresis value and the duration of the shortest pulse (14), which affects the quality of the output signal produced by the controller. In addition, the timing of the first pulse in the controlled variable is identical in both characteristics, as described in (16).

5.3. Impact of deadband and hysteresis

An experimental analysis of the step response was carried out for several controller parameters to further evaluate the controller's performance. The control system's quality was analysed in the time domain using the following parameters [13]: steady-state error (e_{st}), overshoot (κ), and settling time (T_{set}). Moreover, the *integral of the square of the error* (ISE) was chosen as the metric for an overall assessment of the system's quality. It has the following form

$$I_{\mathrm{ISE}} = \int_0^{\infty} \mathrm{d}t\ e^2(t). \tag{17}$$

Performance metrics specific to relay systems were also determined. These include the number of times the setpoint has changed, defined as n_{imp}, and the energy consumption of the system, represented by the duty factor

$$k_w = \frac{t_{on}}{t_{on} + t_{off}} 100\%, \tag{18}$$

where: t_{on} — pulse active time, $t_{on} + t_{off}$ — pulse period.

The hysteresis value h was assumed to be constant and smaller than the smallest value of the deadband a. Based on the responses studied, the performance index values are given in Table I, which also includes the ratio $(\frac{h}{a})$. A constant power factor B was also assumed for the first series of measurements. The simulation time was set to 300 s, and the responses obtained exhibited damped oscillations.

Figure 5 shows the step response of the 3P step controller with the system described in (15). A significant advantage of the 3P-S controller was the nature of the responses obtained. Further simulations were carried out, and even with a very small deadband width $a = 0.045$ and a tenfold increase in the power factor $B = 0.05$, the responses did not reach steady oscillations. The ISE oscillated between 47 and 52 in all cases.

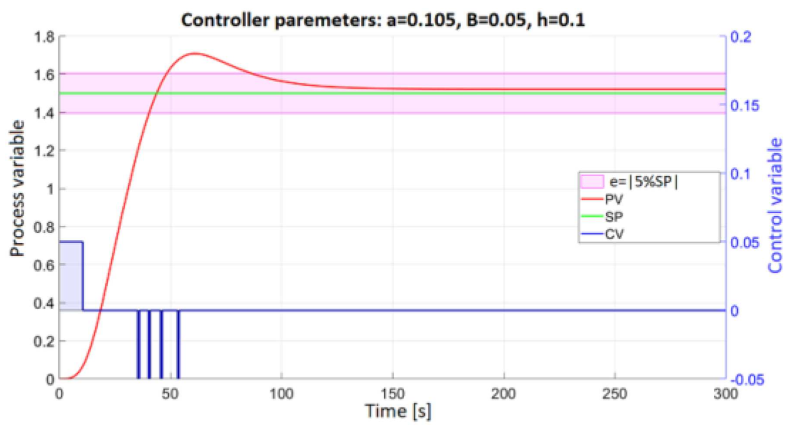

Fig. 5. Example of step response for 3P-S controller.

Controllers with the same hysteresis values h and a higher quality coefficient k_j gave better control results. However, a too-high ($\frac{h}{a}$) ratio of the hysteresis band value to the deadband value (well above 0.5) resulted in poorer performance despite the higher k_j value. In addition to the coefficient a, which determines the possible range of the steady-state error e_{st}, it was found that a particularly important parameter affecting steady-state accuracy is the duration of the shortest pulse (14). Shorter control signal pulses, achieved in this case by minimising the size of the hysteresis band by 0.5, resulted in a smaller steady-state error. However, as expected, the number of pulses in the output variable increased (Fig. 4).

The responses obtained with higher values of the hysteresis band also showed greater overshoot, attributed to the delayed occurrence of the first change in the control signal.

5.4. Impact of power coefficient

Another parameter that has been analysed is the power factor B. It is important to emphasise that the value of the power factor B and the ability to manipulate it are directly related to the dynamics of the drive, allowing the limits of B to be defined. For example, in DC electric drives, a common method of modifying the dynamics is using *pulse-width modulation* (PWM), and in electrohydraulic servo drives, changing the power factor B is possible by adjusting the settings on the throttle valves. However, this approach only sometimes allows to reach the full energy potential of the actuator utilised.

In the second experiment, the controller parameters were set to $a = 0.075$ and $h = 0.05$, with a simulation time of 300 s. Based on the simulations, the performance metrics were determined and summarised in Table II. The results show a direct relationship between the settling time and the value of B. This relationship results from the fact that the rise time of the process value is related to the amplitude of the control value. A shorter settling time was observed for higher power factor B, but this is not a linear relationship. Therefore, a further analysis of the feedback signal was carried out (Fig. 6), which explains the lack of linear correlation between settling time and power factor B.

An increase in the overshoot value can be associated with an increase in parameter B. However, for higher power factor B values, the first control pulse is shortened due to the corrective feedback. At the lowest value of the coefficient B, the lowest overshoot was also observed, while at subsequent values, the overshoot remained at a similar level. Due to the longer control time and the larger steady-state error, the highest value of the ISE index was also obtained for the lowest $B = 0.01$.

The number of control pulses (n_{imp}) decreased significantly with the reduction in power factor B. It is a very beneficial feature as it reduces wear on the actuators.

The duty cycle of the control signal (k_w) has also changed. The control system for higher amplitude pulses proportionally shortens their duration, resulting in similar integrated values of the control signal for $0.1 \leq B \leq 10$ (Fig. 6). The main difference is in the first pulse duration when the changeover occurs. However, the larger the B, the smaller the difference in response. The analysis of the k_w supports this conclusion; for a tenfold increase in B, the duty cycle (and, therefore, the total pulse duration) is reduced by a factor of ten.

The critical parameter highlighted in Table II is $(t_w)_{\min}$. In the experiment $1.6 \leq (t_w)_{\min} \leq 44$ ms. If the control value does not adhere to the set time rigorously, oscillations in the system response may occur.

When implementing a 3P-S controller using a PLC, it is essential to ensure that the programme's control loop operates at a suitable frequency to generate such short control pulses. The implementation

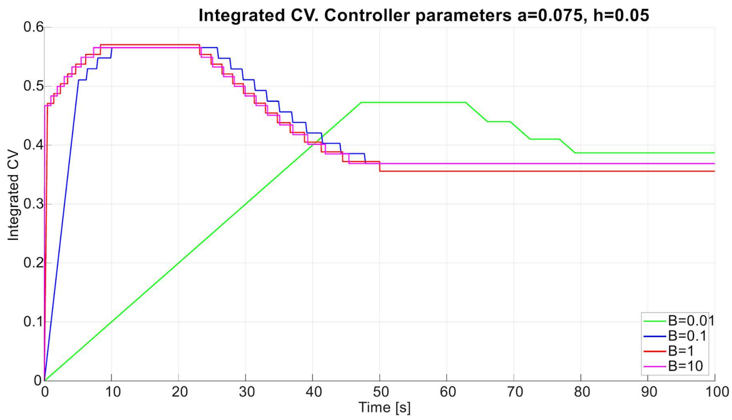

Fig. 6. Integrated signal of control variable for two different values of power factor B.

of the control system, as well as the actuator, can limit the efficiency of the 3P-S controller. It is, therefore, important to analyse the structure of the control system and the expected duration of the shortest control pulses before selecting the system components.

To combine the advantage of a large power factor B, resulting in a shorter settling time, with the benefits of fewer control pulses and an increased minimum duration for smaller values of parameter B, a step change in the value of the coefficient B as a function of the control deviation e can be proposed. If the deviation is sufficiently small, the power factor can be reduced (e.g., a step change in the PWM signal feeding the DC motor), which may have the additional benefit of reducing energy consumption by minimising the need for process inversion (e.g., the DC motor may require reverse polarity of the power supply and braking).

This proposed implementation could be particularly important for the actuators under consideration. In the case of shaft position control, where the setpoint is almost unlimited, the control time for two different power factor values will increasingly diverge as the setpoint increases.

TABLE II

Performance parameters for a 3P step controller for different settings of power factor B.

Controller parameters: $a = 0.075$, $h = 0.050$				
B	0.01	0.10	1.00	10.00
k_j	43.66	4.37	0.44	0.044
$(t_w)_{\min}$	1.6400 s	0.1640 s	0.01640 s	0.0016 s
I_{ISE}	83.43	41.52	37.60	36.26
κ	7.8%	12.45%	13.10%	12.47%
e_{st}	−0.040	−0.025	−0.080	−0.025
T_{set}	199.4 s	78.0 s	–*	75.7 s
n_{imp}	3	14	19	18
k_w	18.610%	2.500%	0.250%	0.025%

*Steady-state error was greater than 5% of SP

deadband also helps to limit overshoot. Therefore, when determining the appropriate size of the deadband, a balance must be struck between the quality of the system response and the number of control pulses n_{imp}.

6. Discussion of results

6.1. The influence of deadband

The experiments show that reducing the size of the deadband a leads to a reduction in the overall error as measured by the IISE. For controllers with a steady-state error, limiting the deadband is beneficial because there is a relationship between the deadband size and the steady-state error range (6). Specifically, the steady-state error is contained within a zone twice the width of the deadband a. However, the value of the deviation is influenced by additional factors such as initial conditions, setpoint, and power factor B. The smaller deadband also helps to limit overshoot. Therefore, when determining the appropriate size of the deadband, a balance must be struck between the quality of the system response and the number of control pulses n_{imp}.

6.2. The influence of hysteresis band

The influence of the hysteresis band h on the resulting responses should be considered in the context of the plant dynamics. The key point is to consider hysteresis not as an absolute value but in relation to the size of the deadband a. For 3P-S controllers, hysteresis is directly proportional to the duration of the shortest control pulse $(t_w)_{\min}$. Unlike the power factor B, hysteresis is a plant-independent parameter, i.e., it can be adjusted within almost any limits.

However, it is important to note that there is no general rule regarding the influence of the hysteresis band h on the system response. Further analysis is required to determine the effects of introducing hysteresis into the system. This analysis must be based on a thorough understanding of the system dynamics.

7. Conclusions

Based on the experiments conducted, the effectiveness of using a 3P-S controller to control systems with complex plant dynamics has been demonstrated with satisfactory results. General guidelines for selecting the settings of 3P-S controllers have been established, allowing the initial determination of the settings based on the step responses of the systems.

- Performance of 3P-S controller: The 3P-S controller, with its corrective feedback loop, enhances control in delayed systems with the integrator part, offering PI-like performance under certain conditions.
- Impact of deadband: Reducing the deadband improves accuracy by decreasing steady-state error and limiting overshoot, but may increase control pulses, requiring a balance to avoid actuator wear.
- Influence of hysteresis band: The hysteresis band impacts pulse duration, stability, and responsiveness; a larger hysteresis stabilises the system but may increase overshoot and reduce accuracy.
- Influence of power factor: Increasing the power factor shortens settling time but raises overshoot and steady-state error. It improves response speed but may increase control pulses, requiring careful tuning to avoid oscillations.

This work can serve as a basis for future research to develop self-tuning algorithms for 3P-S controllers.

References

[1] H. Berger, *Automating with STEP 7 in LAD and FBD: SIMATIC S7-300/400 Programmable Controllers* 5th Ed., Wiley, 2012.

[2] M. Stewart, *Surface Production Operations*, Gulf Professional Publishing, 2019.

[3] T. Milliff, Z. Sun, T. Patel, J. Munich, J. Hill, G. Fields, “Scroll Compressor With Three-Step Capacity Control”, Application number: US20090357580 20090122 (A1), 2009.

[4] Q. Zhong, E. Xu, G. Xie, X. Wang, Y. Li, *Chinese J. Aeronaut.* **36**, 445 (2023).

[5] M.P. Kazimierzowski, R. Krishnan, F. Blaabjerg, *Control in Power Electronics*, Academic Press, 2002.

[6] G.J. Thaler, M.P. Pastel, *Analysis and Design of Nonlinear Feedback Control Systems*, Literary Licensing, 2012.

[7] M. Bartyś, in: *Mechatronics 2017. Advances in Intelligent Systems and Computing*, Vol. 644, Eds. T. Březina, R. Jabłoński, Springer, Cham 2018.

[8] D. Holejko, W. Kościelny, *Automatyka Procesów Ciągłych*, OWPW, Warsaw 2012 (in Polish).

[9] M. Żelazny, *Podstawy Automatyki*, PWN, Warsaw 1976 (in Polish).

[10] R. Isermann, *Digital Control Systems*, Springer, New York 2013.

[11] D. Liberzon, *Switching in Systems and Control*, Vol. 190, Birkhauser, Boston 2003.

[12] S.Y. Nof, *Springer Handbook of Automation* Springer, Berlin 2009, p. 1379.

[13] J. Możaryn, K. Malinowski, in: *Mechatronics 2013: Recent Technological And Scientific Advances* Springer International Publishing, 2014, p. 677.